Photochemical Processing of Dissolved Organic Matter in Fog Water: Oxidation and Functionalization Pathways Driving Organic Aerosol Evolution

Wenqing Jiang^{1,2}, Lijuan Li^{1,3}, Lu Yu^{1,2}, Hwajin Kim^{1,4}, Yele Sun^{1,5}, Qi Zhang^{1,2}*

- ⁵ Department of Environmental Toxicology, University of California, 1 Shields Ave., Davis, CA 95616, USA
 - ²Agricultural and Environmental Chemistry Graduate Group, University of California, 1 Shields Ave., Davis, CA 95616, USA ³Research Center for Atmospheric Environment, Chongqing Institute of Green and Intelligent Technology, Chinese Academy of Sciences, Chongqing 400714, China
 - ⁴Department of Environmental Health Sciences, Seoul National University, Seoul 08826, South Korea
- State Key Laboratory of Atmospheric Environment and Extreme Meteorology, Institute of Atmospheric Physics, Chinese Academy of Sciences, Beijing 100029, China

Corresponding to: Qi Zhang (dkwzhang@ucdavis.edu)

Abstract. Photochemical reactions of dissolved organic matter (DOM) in atmospheric waters can alter the composition and properties organic aerosols (OA), with implications for climate and air quality. In this study, we investigated the aqueousphase transformation of fog DOM under simulated sunlight using online aerosol mass spectrometry (AMS), offline Orbitrap mass spectrometry with electrospray ionization, UV-vis spectroscopy, and aerosol volatility measurements. Irradiation increased the mass concentration of DOM-derived OA (DOM_{OA}), defined as the low-volatility fraction of DOM that forms OA upon water evaporation. This increase was primarily driven by functionalization reactions that added oxygen- and nitrogen-containing groups, as indicated by a stable C mass, rising oxygen-to-carbon (O/C) and nitrogen-to-carbon (N/C) ratios, and enhanced signals of heteroatom-containing compounds over the course of irradiation. Despite evidence of fragmentation, spectral features associated with oligomerization, such as phenolic dimers, were also observed. To characterize chemical aging of fog DOM, we applied positive matrix factorization to the AMS spectra and identified three distinct factors representing progressive stages of aqueous-phase aging: initial DOM_{OA}, more oxidized intermediates, and highly oxidized products, characterized by progressively increasing O/C and N/C ratios. These findings demonstrate that sunlight-induced aqueous-phase oxidation and functionalization of fog DOM drive the formation and aging of secondary OA, altering its composition, volatility, and light-absorbing properties with potential atmospheric consequences.

1 Introduction

2.5

Dissolved organic matter (DOM) is a ubiquitous and chemically diverse component of cloud, fog, and rain droplets, where it plays a central role in the chemical and physical evolution of atmospheric aqueous systems. DOM originates from various sources, including the dissolution of soluble gases, uptake of hygroscopic particles, and multiphase oxidation of hydrophobic compounds into water-soluble forms (Bianco et al. 2020; Collett et al. 2008; Herckes, Valsaraj, and Collett 2013; Kim et al.

2019; Mazzoleni et al. 2010; Pratap et al. 2021; Schneider et al. 2017). As a result, its composition is highly complex (Bianco et al. 2018; Brege et al. 2018; Mazzoleni et al. 2010; Pailler et al. 2024; Sun et al. 2021; Zhao, Hallar, and Mazzoleni 2013), encompassing both small polar molecules (e.g., organic acids, carbonyls, dicarbonyls, and organosulfates) (K E Altieri, Turpin, and Seitzinger 2009; Boris et al. 2018; Herckes, Hannigan, et al. 2002; Liu et al. 2021; Pratt et al. 2013) and high molecular weight (HMW) species such as humic-like substances and secondary oligomers (K E Altieri et al. 2009; Collett et al. 2008; Hawkins et al. 2016; Laskin, Laskin, and Nizkorodov 2015; Renard et al. 2015; Sun et al. 2010). Primary particle tracers, such as n-alkanes, long-chain alkanoic acids, and polycyclic aromatic hydrocarbons (PAHs), have also been detected in fog and cloud droplets, though they typically represent only a minor fraction of dissolved carbon, even in heavily polluted areas (Collett et al. 2008; Ehrenhauser et al. 2012).

In addition to carbon-rich compounds, organic nitrogen (ON) and organic sulfur (OS) species are also prevalent in atmospheric waters. These include amines, N-containing heteroaromatics, nitrophenols, and nitrooxy-organosulfates (Katye E Altieri, Turpin, and Seitzinger 2009; Desyaterik et al. 2013; Kim et al. 2019; Mattsson et al. 2025; Sun et al. 2024; Youn et al. 2015; Zhang and Anastasio 2003b; Zhang, Anastasio, and Jimenez-Cruz 2002), particularly in regions impacted by biomass burning and agricultural emissions (Collett et al. 2008; Li et al. 2023; Mattsson et al. 2025; Parworth et al. 2017; Zhang and Anastasio 2001). ON and OS species can enter cloud and fog droplets via direct uptake of gaseous or particulate species, or they may form secondarily through aqueous-phase reactions involving precursors such as ammonia, amines, amino acids, and SO₂.

A wide range of VOCs (e.g., isoprene, monoterpenes, glyoxal, methylglyoxal, and phenols) contribute to DOM via gas-to-

liquid partitioning followed by aqueous-phase reactions (Arciva et al. 2022; Ervens et al. 2008; Jiang et al. 2021; Tomaz et al. 2018; Wang et al. 2021; Yu et al. 2014; Zhang et al. 2024). These VOCs, along with pre-existing DOM, can undergo direct photolysis or react with a suite of oxidants, including hydroxyl radical (•OH), singlet oxygen ($^{1}O_{2}^{*}$), hydrogen peroxide, peroxyl radicals, ozone (O_{3}), nitrate radical (•NO₃), sulfate radical (•SO₄-), and organic triplet excited states ($^{3}C^{*}$) (Bianco et al. 2020; Borduas-Dedekind et al. 2019; Hems et al. 2020; Herrmann et al. 2015; Jiang et al. 2023; Kaur et al. 2019; Smith, Kinney, and Anastasio 2015; Tomaz et al. 2018; Zhang and Anastasio 2003a). These reactions significantly alter the aqueous phase composition and, following droplet evaporation, influence the concentration, oxidation state ($O_{S_{C}}$), and molecular makeup of the resulting organic aerosols ($O_{S_{C}}$) (Farley et al. 2023; Hems et al. 2020; Kim et al. 2019; Lee et al. 2012; Renard et al. 2015; Schneider et al. 2017; Schurman et al. 2018). Consequently, aqueous-phase processing of DOM affects OA's light absorption and cloud activation properties, with broad implications for atmospheric chemistry and Earth's radiative budget (Borduas-Dedekind et al. 2019; Farley et al. 2023; Hems et al. 2020).

55

Despite growing recognition of the importance of aqueous-phase chemistry, significant knowledge gaps remain regarding the evolution of real-world DOM under ambient atmospheric conditions. These uncertainties limit our ability to predict aerosol-cloud interactions, which represent one of the largest sources of uncertainty in climate models. While laboratory studies have yielded valuable mechanistic insights, they often rely on simplified model systems that don't capture the chemical complexity of ambient DOM. Other studies using real-world samples often employed non-atmospheric irradiation (e.g., 254 nm UV), reducing their relevance to atmospheric processes.

In this study, we examine the photochemical transformation of DOM in wintertime fog water collected in Fresno, California – a major urban center in the San Joaquin Valley (SJV), where fog plays a key role in winter aerosol pollution. The SJV has been the subject of extensive fog chemistry research (Collett et al. 2001; Collier et al. 2018; Ehrenhauser et al. 2012; Ge, Zhang, et al. 2012; Herckes et al. 2015; Kim et al. 2019; Zhang and Anastasio 2001), and Fresno fog water is known to contain a complex mixture of organic compounds spanning a wide range of chemical properties (Herckes, Leenheer, and Collett 2007; Kim et al. 2019; Mazzoleni et al. 2010; Zhang and Anastasio 2001). Here, we define "DOM" as the total pool of dissolved organics, including water-soluble gases, and "DOM_{OA}" as the low-volatility fraction that remains in the particle phase after fog water aerosolization and drying. We used a high-resolution time-of-flight aerosol mass spectrometer (HR-AMS) to track DOM_{OA} concentration and composition in real time during simulated sunlight illumination. Positive matrix factorization (PMF) was applied to the HR-AMS spectra to resolve distinct stages of aqueous-phase aging, complemented by molecular analysis using Orbitrap mass spectrometry with electrospray ionization (ESI-MS), UV-Vis spectroscopy, and thermodenuder measurements of aerosol volatility.

2 Experimental methods

2.1 Collection of fog water samples

The fog water samples were collected on Jan 9, 2010, in Fresno in the SJV of California, as detailed in Kim et al. (Kim et al. 2019). The sampling site was situated at a large agricultural field of California State University, Fresno (36o49'35.9"N, 119o44'42.7"W), in relatively close proximity to two major highways and a residential area (Ehrenhauser et al. 2012; Wang et al. 2013). Fog samples were collected using Caltech Active Strand Cloud Collectors (CASCC; ~ 25.4 m³ min⁻¹ airflow) (Demoz, Collett, and Daube 1996) and a stainless steel extra-large CASCC collector (XL-CASS; ~ 40 m³ min⁻¹ air flow) (Herckes et al. 2007). All samples were immediately filtered onsite using 0.22 µm glass fiber filters (Wang et al. 2013) and stored in the dark at ~20 °C until analysis. Fog sample characteristics were previously reported by Kim et al. (2019) and are summarized in Table S1. Three consecutive fog samples with highly similar chemical composition were combined to yield approximately 110 mL of composite sample for photooxidation experiments conducted in February 2015. Although multiyear storage can potentially affect certain labile compounds, these samples were also analyzed shortly after collection, with results reported in Kim et al. (2019). The HR-AMS spectrum of the unilluminated fog sample from this study is highly similar to the spectra reported by Kim et al. (2019), indicating that DOM_{OA} composition remained largely unchanged during storage. Additionally, the composition of the fog samples used in this study is similar to other winter fog water samples from Fresno and Davis, CA (Kim et al., 2019), confirming its representativeness for winter fogs in California's Central Valley.

95 2.2 Photochemical oxidation

100

105

110

115

120

Aqueous oxidation was carried out using air-saturated fog water stirred in a Pyrex tube and exposed to simulated sunlight inside an RPR-200 Photoreactor System equipped with three types of bulbs emitting wavelengths of light centered at 300, 350 and 419 nm, respectively. Fig. S1 shows the normalized photon fluxes inside the RPR-200 illumination system. In this setup, lamp emission below 315 nm is minimal, and the Pyrex tube further blocks wavelengths below 300 nm, effectively confining the actinic flux reaching the solution to the UVA and visible range. No additional optical filters were employed. Prior actinometry measurements of this RPR-200 illumination system indicate that its photochemical rate is ~7 times faster than that of winter solstice midday sunlight in Northern California (George et al., 2015). Accordingly, the ~8 h of illumination applied in our photochemical experiments corresponds to approximately 56 h of exposure to ambient sunlight. Under this condition, a variety of oxidants, such as hydroxyl radical (•OH), nitrate radical (•NO₃), triplet states of organic carbon (³C*), and singlet molecular oxygen (${}^{1}O_{2}^{*}$), can be produced during illumination and react with dissolved organics in the aqueous phase. ${}^{3}C^{*}$ can form when brown carbon chromophores in fog water absorb light and undergo intersystem crossing (McNeill and Canonica 2016). Energy transfer between ³C* and dissolved O₂ yields ¹O₂* (Kaur and Anastasio 2017; Ossola et al. 2021). H₂O₂ can be generated via energy/electron transfer of ³C* (Anastasio, Faust, and Rao 1997), which can subsequently undergo photolysis to produce •OH. Additionally, •OH can be generated from nitrate and nitrite photolysis in fog water (Brezonik and Fulkerson-Brekken 1998). Previous studies have reported steady-state •OH concentration in fog water from Northern California (winter sunlight) in the range of $3.4-6.6\times10^{-16}$ M, and ${}^{1}O_{2}^{*}$ concentration of $1.1-6.1\times10^{-13}$ M (Anastasio and McGregor 2001). A Shimadzu LC-10AD high-performance liquid chromatography pump continuously drew solution at a flow rate of 0.2 mL min ¹ from the illuminated tube or a dark control tube wrapped entirely with aluminum foil. The effluent was atomized with nitrogen, fully dried using a diffusion dryer, and analyzed in real-time by HR-AMS. The non-refractory organics detected after this atomization-drying process are defined as DOM_{OA}, while compounds that completely volatilize during drying are not included. This nebulizer-dryer-AMS approach has been widely used in prior fog studies (Brege et al., 2018; Kim et al., 2019; Mattsson et al., 2025). The illuminated solution was continuously aerosolized and sampled until fully consumed, which took ~ 8 hours. Additionally, aliquots of the illuminated fog water samples were collected over four consecutive time intervals (S1: 0-2 h, S2: 2-4 h, S3: 4-6 h, and S4: 6-8 h) and analyzed offline by electrospray ionization mass spectrometry (ESI-MS) and UV-vis spectroscopy.

2.3 HR-AMS measurement and data analysis

2.3.1 HR-AMS measurement and data analysis

Bulk chemical composition and elemental ratios of DOM_{OA} were analyzed using the HR-AMS, which employs 70 eV electron ionization (EI) mass spectrometry after aerosol evaporation at ~ 600 °C (DeCarlo et al. 2006). The instrument was operated in both "V" and "W" ion optical modes, achieving mass resolutions of ~ 3000 and ~ 5000 , and capturing spectra up to m/z 500 and 300 amu, respectively.

HR-AMS data were processed using SQUIRREL v1.15 and PIKA v1.56 (available at http://cires.colorado.edu/jimenez-group/ToFAMSResources/ToFSoftware/). W-mode data were used to obtain high-resolution mass spectra (HRMS) and derive elemental ratios, including oxygen-to-carbon (O/C), hydrogen-to-carbon (H/C), nitrogen-to-carbon (N/C), sulfur-to-carbon (S/C), and the organic mass-to-carbon ratio (OM/OC) (Aiken et al. 2008). With relative humidity at the HR-AMS inlet below 5%, contributions from water vapor were considered negligible, and the organic H_2O^+ signal was estimated by subtracting the sulfate-derived contribution from the total H_2O^+ signal (Allan et al. 2004). To estimate the organic CO^+ signal, we performed a separate, offline HR-AMS analysis of fog samples using argon as the atomization gas (Yu et al. 2014), which eliminates the interference from N_2 at m/z 28. The argon-atomized measurements showed that the CO^+ signal was ~ 31% as intense as the CO_2^+ signal in DOM_{OA} mass spectra. This ratio (CO^+ = 0.31 × CO_2^+) was then applied to the online N_2 -atomized HR-AMS data to improve the accuracy of DOM_{OA} O/C and OM/OC estimates.

2.3.2 Positive Matrix Factorization (PMF) analysis

130

135

140

145

150

PMF analysis was performed using the PMF2.exe algorithm in robust mode (Paatero and Tapper 1994), via the PMF Evaluation Toolkit (PET) v2.06 (Ulbrich et al. 2009), available at http://cires.colorado.edu/jimenez-group/wiki/index.php/PMF-AMS_Analysis_Guide. The input data included the ion-speciated HRMS matrix (containing 287 ions and 1001 time points) and its corresponding error matrix, prepared following the refinement protocol outlined in Table 1 of Zhang et al. (Zhang et al. 2011).

To identify the optimal solution, PMF was run using factor numbers (p) from 1 to 5 and rotational parameters (fPeak) from 1.0 to 1.0 in 0.1 increment, as recommended by Zhang et al. (Zhang et al. 2011). After a thorough examination, the 3-factor solution with fPeak = -0.1 ($Q/Q_{exp} = 5.57$) was chosen. A summary of key diagnostic plots is presented in Fig. S2 in the supplementary materials. This solution best captured both the total DOM_{OA} mass and its temporal evolution (Fig. S2f), with only minor variations across different fPeak values (Fig. S2c). For comparison, the 2-factor and 4-factor solutions are shown in Fig. S3, with diagnostics in Figs. S4–S5. The 2-factor solution underperformed during the initial irradiation phase, while the 4-factor solution split one interpretable component into two less meaningful factors. Overall, the 3-factor solution provided the most robust and interpretable description of DOM_{OA} evolution under simulated sunlight.

2.4 Determination of DOM_{OA} formation and decay rates for the three PMF factors

The formation and decay kinetics of DOM_{OA} associated with the three PMF factors were determined through curve fitting using Igor Pro 6.36 (Wavemetrics, Portland, OR, USA). The temporal evolution of each factor was modelled using exponential functions. The decay of Factor 1 was fitted using a pseudo first-order kinetic model:

$$[DOM_{0A-fac1}]_t = a + b \cdot \exp(-k_d t)$$
 (1)

For Factor 2, both formation and decay processes were considered and modeled using a double exponential function:

$$[DOM_{OA-fac2}]_t = a + b \cdot \exp(-k_f t) + c \cdot \exp(-k_d t)$$
 (2)

The formation rate of Factor 3 was modeled as a first-order process driven by the decay of Factor 2:

$$[DOM_{OA-fac3}]_t = a + b \cdot exp(-k_f t)$$
(3)

Here, $[DOM_{OA-faci}]_t$ is the concentration of the i-th DOM_{OA} factor at time t; a, b, and c are fitted coefficients; k_f and k_d represent apparent first-order formation and decay rate constants, respectively. These parameters were obtained by least-squares fitting the models to the experimental data.

2.5 ESI-MS analysis

165

170

175

180

Fog water samples collected over four irradiation time intervals, corresponding to distinct photochemical aging stages (Fig. S6), were analyzed using an LTQ Orbitrap mass spectrometer (Thermo Scientific, Inc.) equipped with an electrospray ionization (ESI) source operated in positive mode for molecular characterization. Winter fog DOM in Fresno is characterized by high N/C ratios and elevated concentrations of N-containing organics, such as amines, amino acids and imidazoles (Kim et al., 2019), which are protonatable and exhibit strong sensitivity in positive-mode ESI. Given our interest in formation and transformation of organic nitrogen species, we analyzed the samples in positive mode. Mass spectrometry data were acquired using Xcalibur software, and individual MS peaks with signal-to-noise ratio (S/N) > 10 were extracted using the Decon2LS program. Subsequent processing and formula assignments were conducted with customized Microsoft Excel macros (Roach, Laskin, and Laskin 2011) based on Kendrick mass (KM) defect analysis with a KM base of CH₂, excluding ¹³C isotopes. Formula assignments were restricted by a mass accuracy threshold of < 5 ppm and the following elemental limits: $C \le 100$, $C \le$

3. Results and discussion

3.1 Photochemical transformation of low-volatility organic species in fog water

Photochemical processing significantly altered the mass concentration and chemical composition of low-volatility organic solutes (DOM_{OA}) in fog water. As shown in Figs. 1d and S7, DOM_{OA} increased from 25% to 38% of total solute mass over ~ 8 hours of simulated sunlight exposure – equivalent to roughly 56 hours of winter solstice midday sunlight in Northern California based on actinometry measurements (George et al. 2015). In contrast, major inorganic species (i.e., nitrate, ammonia, sulfate, and chloride) remained largely unchanged, indicating net production of low-volatility organic compounds via aqueous-phase photochemistry.

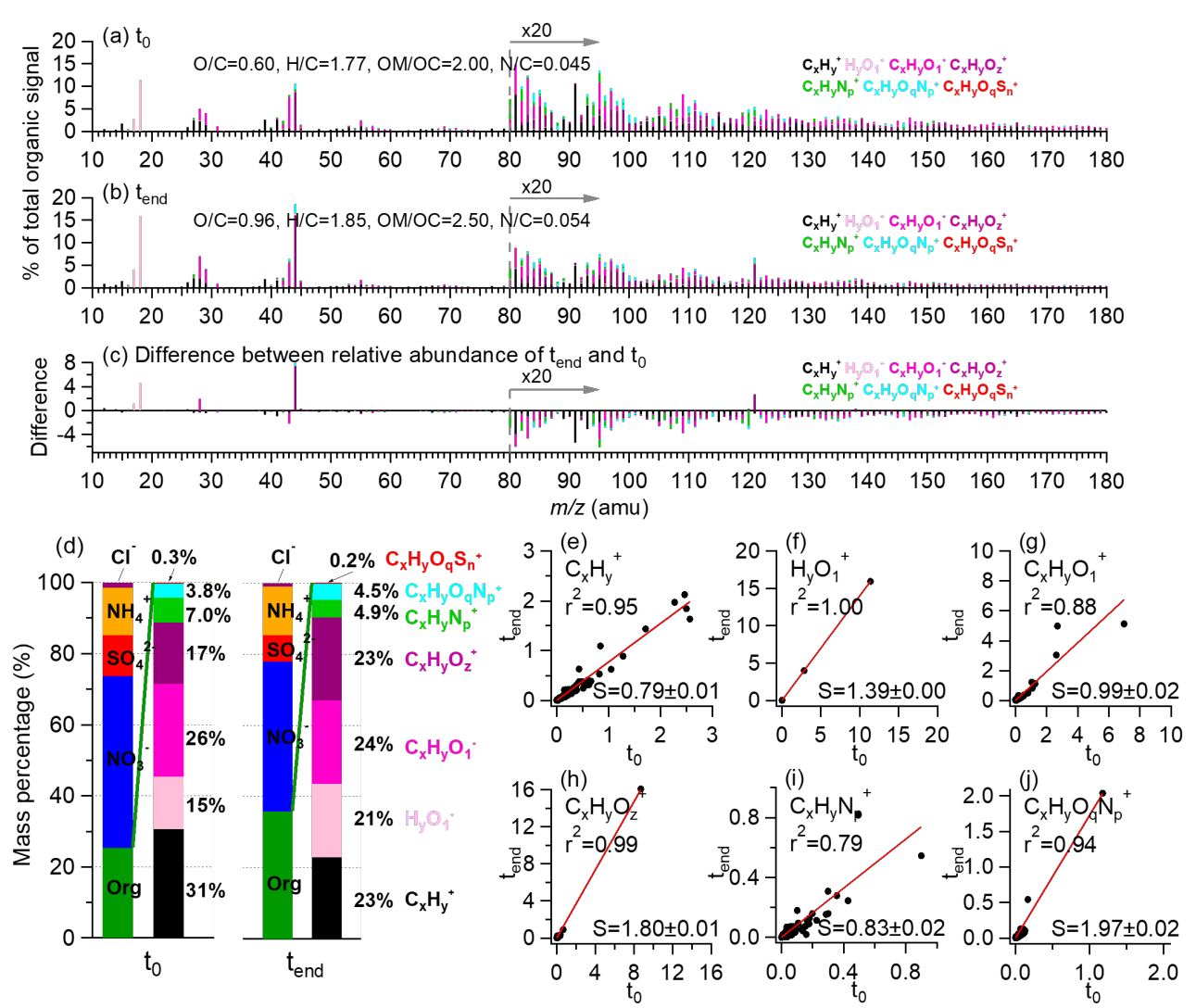


Figure 1. Overview of DOM_{OA} composition before (t₀) and after (t_{end}) eight hours of simulated sunlight illumination. (a-c) HR-AMS spectra of DOM_{OA} at t₀ and t_{end}, and the difference spectrum between them (t_{end} minus t₀), with peaks color-coded by ion categories: C_xH_y⁺, H_yO₁⁺, C_xH_yO_z⁺, C_xH_yO_qN_p⁺, C_xH_yO_qS_n⁺ (x ≥ 1; y ≥ 1; z > 1; p ≥ 1; q ≥ 1; n ≥ 1). Signals at m/z ≥ 80 are multiplied by 20 for clarity. Elemental ratios are noted in the legend. (d) Mass fractions of major inorganic species and DOM_{OA} ion categories at t₀ and t_{end} (colors of ion categories match panels a-c). (e-j) Comparison of each ion category's signal contributions (% of total organic signal) at t₀ and t_{end}. Red lines show orthogonal distance regression (ODR) fits; slopes (S) and correlation coefficients (r²) are provided in each panel.

Irradiation-induced changes in DOM_{OA} composition are evident in the HR-AMS spectra (Figs. 1a-c). The O/C ratio increased from 0.60 prior to illumination (t_0) to 0.96 at t_{end} , and the fraction of CO_2^+ to total organic signal (f_{CO2^+}) increased from 8.5% to 15.5%, reflecting substantial oxidative aging processes. These changes are consistent with ambient wintertime observations in Fresno using real-time HR-AMS (Chen et al. 2018; Young et al. 2016). DOM_{OA} at t_0 resembled less-oxidized oxygenated OA (LO-OOA) and semi-volatile OOA (SV-OOA), while after irradiation it was more similar to more-oxidized OOA (MO-

OOA) and low-volatility OOA (LV-OOA) (Figs. 2d and S8). SV-OOA and LV-OOA are typically representative of relatively fresh and more-aged SOA, respectively (Ng et al. 2010). In addition, the nitrogen-to-carbon (N/C) ratio of DOM_{OA} increased from 0.045 to 0.054, indicating incorporation of nitrogen into the organic matrix, likely through reactions between DOM and N-containing nucleophiles such as ammonia, amino acids, and amines (Haan et al. 2009; Hawkins et al. 2016; Nozière, Dziedzic, and Córdova 2009; Shapiro et al. 2009). The AMS NO₂+/NO+ ratio decreased from 1.37 to 0.72 during illumination (Fig. S9), consistent with formation of low-volatility organic nitrates (Day et al. 2022; Farmer et al. 2010).

200

205

210

215

220

225

Figures 1e-j show scatter plots comparing the contributions of major HR-AMS ion families (i.e., $C_x H_v^+$, $H_v O_1^+$, $C_x H_v O_1^+$, $C_xH_vO_z^+, C_xH_vN_p^+, \text{ and } C_xH_vO_qN_p^+ (x \ge 1; y \ge 1; z > 1; p \ge 1; q \ge 1))$ to the total organic signal at t_0 and t_{end} . The corresponding comparisons of absolute ion signals are shown in Figure S10. In most cases, orthogonal distance regression (ODR) slopes (S) significantly deviated from unity, highlighting systematic chemical evolution of DOM_{OA} during irradiation. The decreases of hydrocarbon-like ions ($C_xH_y^+$, S = 0.79; Fig. 1e) suggest fragmentation of carbon backbones via photooxidation. In HR-AMS, organic-derived H_vO₁⁺ ions are generated during vaporization and ionization of oxygenated organics such as carboxylic acids and alcohols (Canagaratna et al. 2015). In Fig. 1f, $H_vO_1^+$ ions showed a slope of 1.39, suggesting formation of oxygenated organics. The overall fractional contribution of the lightly oxygenated ion family (C_xH_yO₁⁺) remained unchanged during illumination (S=0.99; Fig. 1g). However, several individual ions departed significantly from the 1:1 line, indicating compositional change within the family. In contrast, the relative abundance of more oxygenated ions (C_xH_yO_z⁺; Fig. 1h) increased sharply (S = 1.80), and their tightly correlated spectral patterns at t_0 and t_{end} ($r^2 = 0.99$) suggest formation of highly oxidized species with structural similarity to pre-existing compounds. The dominance of CO₂⁺ and CHO₂⁺ within this family suggests carboxylation as a major pathway. In parallel, reduced organic nitrogen ions ($C_xH_vN_p^+$; Fig. 1i) decreased in relative abundance (S = 0.83), while oxidized organic nitrogen ions ($C_xH_yO_qN_p^+$; Fig. 1j) increased (S = 1.97). Consequently, the $C_xH_vN_p^+/C_xH_vO_qN_p^+$ ratio decreased from 2.1 to 1.2 (Fig. S11), consistent with oxidative transformation and functionalization of ON species during aqueous-phase processing.

Figure 2 illustrates the temporal evolution of DOM_{OA} during irradiation. Its mass concentration increased steadily (Fig. 2a), accompanied by rising O/C and N/C ratios, indicating continuous photochemical transformation. Despite these changes, the total carbon concentration remained nearly constant over 8 hours of irradiation (RSD = 1.3%, Fig. 2a), suggesting minimal carbon loss to the gas phase. While previous studies have reported that ~ 10% of dissolved organic carbon in fog can be small volatiles such as acetate, formate, and formaldehyde (Herckes, Lee, et al. 2002), such VOCs were not detected in our samples (Kim et al. 2019). Although some volatilization during storage is possible, samples were stored in sealed containers at -20 °C in the dark, minimizing reaction losses. As shown in Fig. 2a, the observed DOM_{OA} mass increase was primarily driven by oxygen incorporation, with nitrogen addition playing a lesser role.

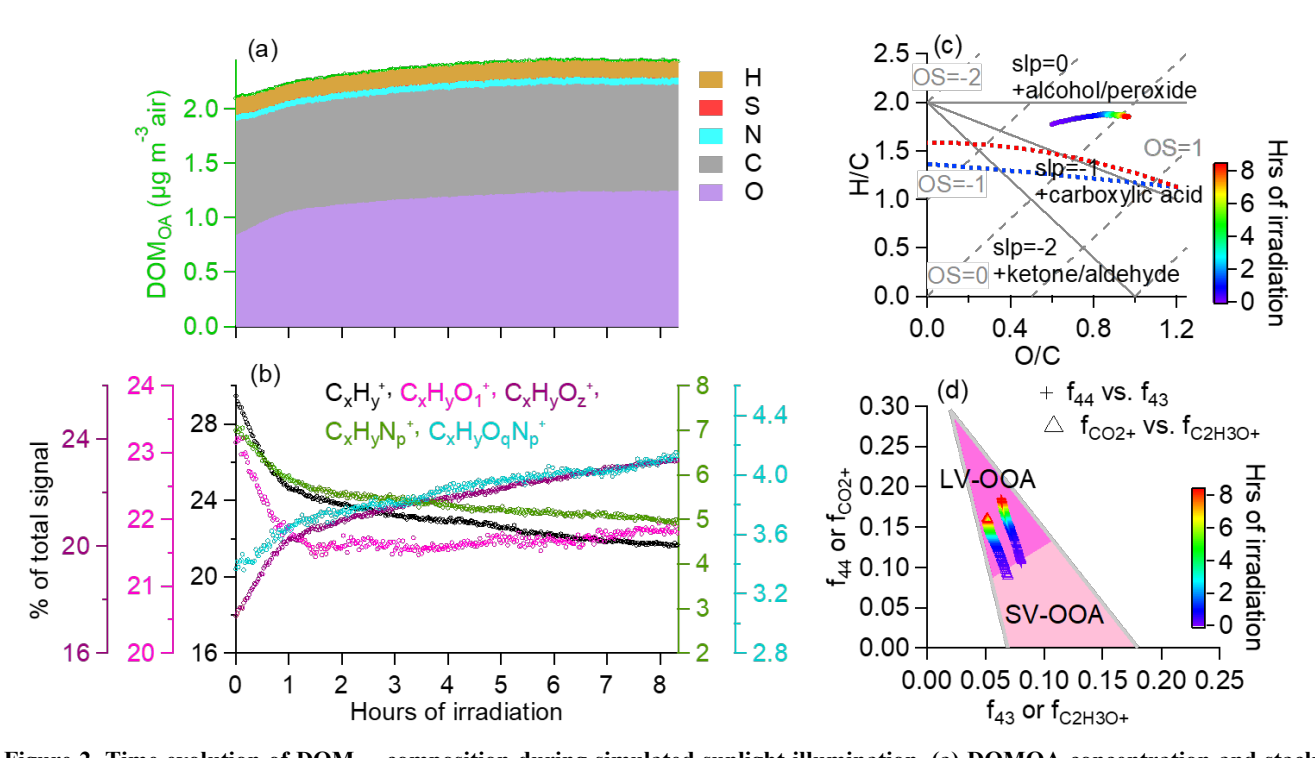


Figure 2. Time evolution of DOMOA composition during simulated sunlight illumination. (a) DOMOA concentration and stacked mass contributions from O, C, N, S and H atoms. The mass concentrations represent ambient air concentrations, calculated by normalizing the liquid-phase concentrations to the sampled air volumes. (b) Fractional contributions of major ion categories to the total DOMOA signals in HR-AMS spectra: $C_xH_y^+$, $C_xH_yO_1^+$, $C_xH_yO_2^+$, $C_xH_yN_p^+$, and $C_xH_yO_qN_p^+$ ($x \ge 1$; $y \ge 1$; z > 1; $p \ge 1$). (c) Evolution profiles of DOMOA in Van Krevelen space based on AMS measurements. (d) Evolution of f44 (fraction of m/z 44 in the AMS organic spectrum), f43 (fraction of m/z 43), fcO2+ (fraction of CO2+ ion) and fc2H3O+ (fraction of C2H3O+ ion). In this study, CO2+ dominates m/z 44 (83%-88%), with minor contributions from C2H6N+ and CH2NO+. C2H3O+ dominates m/z 43, with C3H7+, C2H5N+, and CHNO+ contributing the remainder. The shaded triangle area denotes the region where most ambient oxygenated organic aerosol (OOA) falls into, with the upper-right corner characteristic of low-volatility OOA (LV-OOA) and the lower-right corner of semi-volatile OOA (SV-OOA) (Ng et al. 2010, 2011).

Figures 2b and S12 provide further insights into the photochemical evolution of DOM_{OA} through temporal trends and correlation analysis of five major HR-AMS ion categories. Signals from less oxygenated species $(C_xH_y^+, C_xH_yO_1^+)$ and $C_xH_yN_p^+$ decreased in their contribution to the total organic signal with irradiation, while more oxidized and nitrogen-functionalized categories $(C_xH_yO_z^+)$ and $C_xH_yO_qN_p^+$ increased, indicating progressive oxidation and nitrogen incorporation. The decline in $C_xH_y^+$ reflects the breakdown of aliphatic and aromatic precursors, while the rise in $C_xH_yO_z^+$ and $C_xH_yO_qN_p^+$ is consistent with enhanced oxygenation and functionalization.

Strong negative correlations between $C_xH_y^+$ and both $C_xH_yO_z^+$ and $C_xH_yO_qN_p^+$ support the conversion of less oxidized compounds into highly oxygenated species. Additionally, positive correlations among O- and N-containing ions suggest shared aqueous-phase formation pathways, potentially involving reactions with nitrogenous species such as ammonium, amines, or organic nitrates. Collectively, these results highlight the extensive molecular transformation of DOM_{OA} during photochemical

aging, involving both functionalization and fragmentation, with a net buildup of highly functionalized organics. The evolving HR-AMS ion signatures are consistent with the aqueous-phase formation of SOA-like material under atmospheric conditions.

250 3.2 Insights into photochemical aging pathways of fog DOM

255

260

Photochemical aging of fog DOM involves both fragmentation of high-molecular-weight compounds and formation of highly functionalized, O- and N-containing species, as revealed by complementary ESI-MS and HR-AMS analyses.

Molecular-level insights from positive-mode ESI-MS corroborated the HR-AMS findings. As shown in Fig. S13, the relative abundance of CHN compounds decreased from 7.3% to 3.7% over 8 hours of irradiation, while the CHONS compounds increased from 27.4% to 39.5%. The total CHON fraction remained relatively stable (38.9%–40%), but individual compounds, such as C₉H₁₇NO₈, increased markedly (Fig. 3a), suggesting oxidative conversion of CHN species (e.g., amines, imines, and heterocyclics) into more oxidized forms. The CHN species that decreased during irradiation were primarily C₇ – C₁₆ compounds (Fig. 3c), whereas the CHON increases were mainly driven by C₉ species and the CHONS increases were associated with smaller molecules (e.g., C₂, C₃, C₄, and C₁₁) (Figs. 3f & 3h). These shifts in carbon number indicate fragmentation pathways that produce smaller O-, N-, and S-containing products.

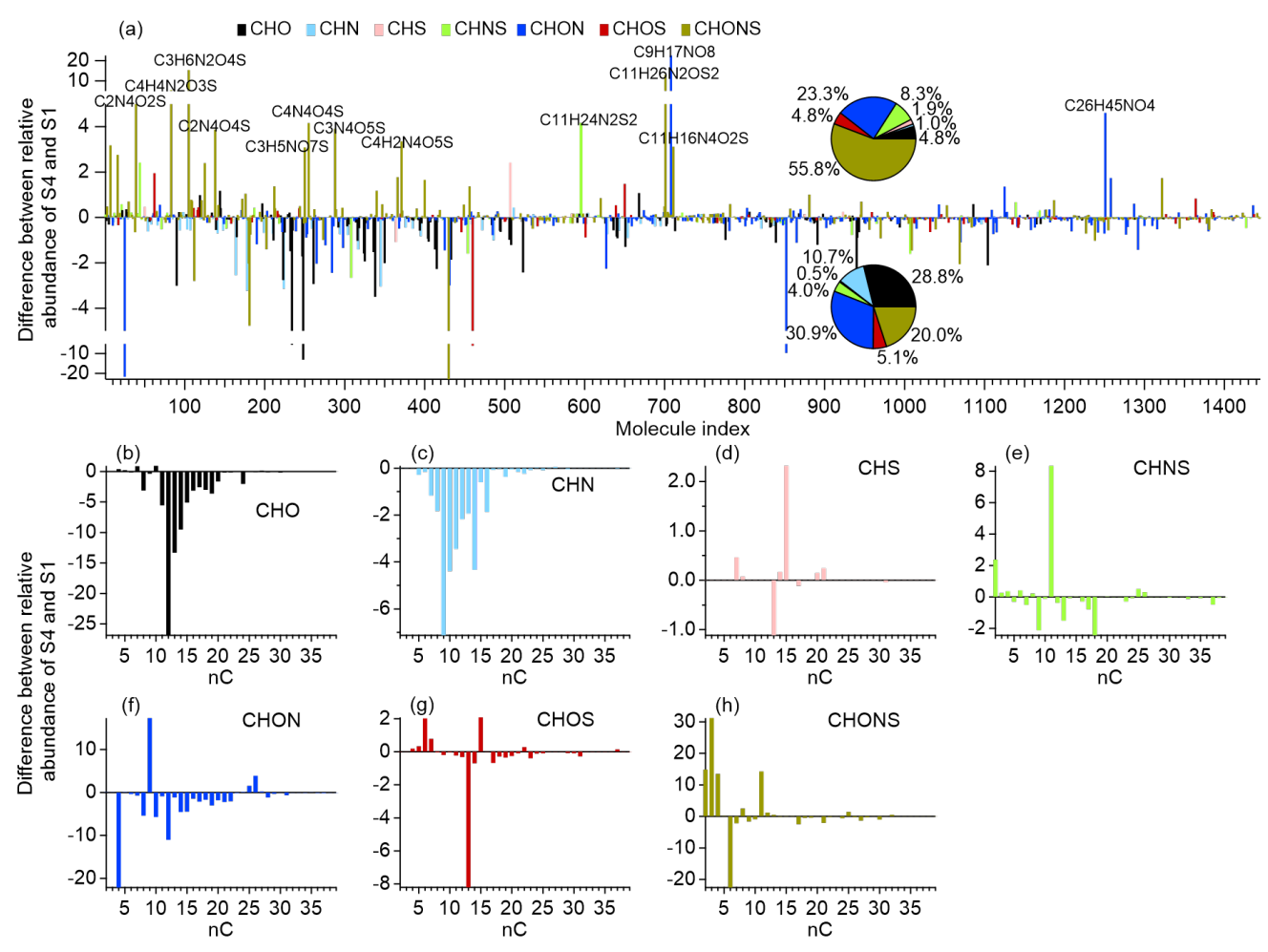
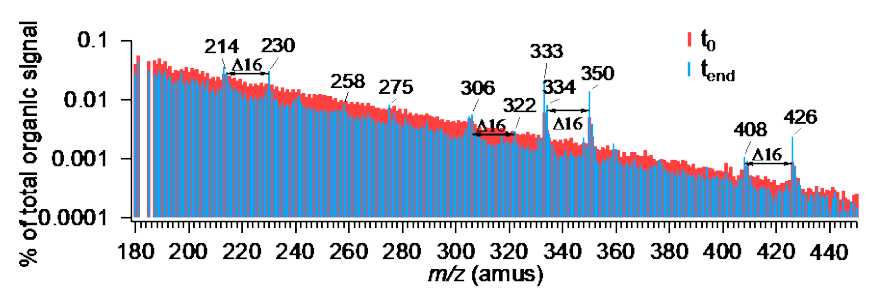


Figure 3. Compositional changes in fog DOM observed by positive-mode ESI-MS between the early (0–2 h, S1) and late (6–8 h, S4) irradiation periods. (a) Difference in relative abundance of all detected molecular formulas between S1 and S4; (b–h) Histograms showing changes in relative abundance of compounds grouped by carbon number for each molecular class: CHO, CHN, CHS, CHNS, CHON, CHOS, and CHONS.

270

Fragmentation was also evident in HR-AMS data, with high-mass ion signals declining after irradiation. As shown in Figure 4, the unit mass resolution (UMR) spectra of DOM_{OA} in the m/z 180–450 range showed widespread signal reductions consistent with the breakdown of HMW species known to present in fog water (Ehrenhauser et al. 2012; Herckes, Lee, et al. 2002; Mazzoleni et al. 2010). However, a set of peaks (e.g., m/z 214, 230, 258, 275, 334, and 350) increased in intensity, with some spaced by 16 amu – indicative of progressive oxygen addition through reactions such as hydroxylation, peroxide formation, or radical-mediated reactions. This interpretation is also supported by the evolution of H/C and O/C ratios in Van Krevelen space (Fig. 2c), which follows a near-zero slope, consistent with net oxygen incorporation. Additionally, the fractional contribution of CHO₂⁺ to the total organic signal gradually increased from 0.63% to 0.93% during irradiation (Fig. S14), suggesting that carboxylation played an important role in the formation of functionalized products. High-resolution peak fitting

of these increased ions indicates that they either contain nitrogen or consist solely of C, H and O (Fig. S15). These results imply that photochemical aging of fog DOM involves both loss of HMW compounds and formation of new functionalized products.



280

285

290

295

300

Figure 4. Comparison of unit mass resolution (UMR) spectra of DOM_{OA} in fog water before (t₀, blue) and after (t_{end}, red) simulated sunlight illumination, over the *m/z* range 180–450 amu.

Notably, the *m/z* 306 signal, a known tracer ion for syringol dimer formation (Sun et al. 2010; Yu et al. 2014), was enhanced following irradiation. Syringol, a methoxyphenol commonly emitted during biomass burning, is likely present in the fog water due to winter residential wood burning in the region (Chen et al. 2018; Ge, Setyan, et al. 2012; Young et al. 2016). The enhancement of *m/z* 306 provides direct evidence of aqueous-phase oligomerization of biomass burning-derived phenolic precursors, consistent with prior laboratory (Huang et al. 2018; Jiang et al. 2021, 2023; Yu et al. 2016) and field studies showing photooxidation of phenolics leads to hydroxylation, ether formation, and oligomerization (Gilardoni et al. 2016). Together, these findings highlight the dual role of aqueous-phase photochemistry: simultaneous fragmentation of existing DOM and generation of new, more oxygenated species with enhanced functionality. The concurrent increases in oxidation and nitrogen incorporation are consistent with aqueous-phase aging pathways that produce SOA-like material enriched in O- and N-functional groups.

3.3 Characterizing aqueous phase photoaging of DOM_{OA} via PMF

We applied PMF to the HR-AMS spectra to further resolve the progressive aqueous-phase aging of DOM_{OA} during simulated sunlight irradiation. This analysis allows us to deconvolve overlapping transformation processes and link them to chemical composition and reactivity. Three distinct factors were identified (Fig. 5), each corresponding to a different stage of photochemical processing. Factor 1 represented the initial DOM_{OA}, characterized by O/C = 0.66, H/C = 1.82, OS_C = -0.5, and N/C of 0.036. Its mass spectrum closely matched that of the bulk DOM_{OA} at t_0 . This factor decayed rapidly, with a first-order loss rate constant of k_d = 2.0 hr⁻¹. Factor 2 emerged shortly after the start of illumination and peaked around 1.5 hours, increasing with a formation rate constant of k_f = 2.6 hr⁻¹ before gradually declining at k_d = 0.016 hr⁻¹. This intermediate factor exhibited increased oxidation (O/C = 0.96) and a slightly higher N/C (= 0.038) compared to Factor 1, indicating the incorporation of oxygenated functional groups into DOM. The transient nature and intermediate oxidation level of Factor 2 imply that it represented a key transformation stage, where precursor molecules were actively undergoing aqueous-phase

reactions, likely including hydroxylation, carbonyl formation, and nitrogenation (Hawkins et al. 2016; Herrmann et al. 2015; Renard et al. 2015), on their way to forming more stable, low-volatility products.

305

310

Factor 3, the most oxidized component with the highest O/C (1.12) and N/C (0.040) ratios, accumulated gradually throughout the irradiation period, with an estimated formation rate constant of k_f = 0.13 hr⁻¹. This factor was enriched in highly oxygenated fragments (e.g., $C_xH_yO_z^+$), including ions such as CO_2^+ and CHO_2^+ , which are markers for carboxylic acids and other highly oxidized organic compounds. The elevated N/C ratio of Factor 3 (0.040 vs. 0.036 for Factor 1) indicates nitrogen incorporation into DOM_{OA} during photochemical aging. This conclusion is supported by multiple observations: over illumination, the low-volatility nitrogen mass increased from 0.055 to 0.062 μ g mr⁻³; the N/C ratio of DOM_{OA} increased from 0.045 to 0.054; and the AMS NO₂⁺/NO⁺ ratio decreased from 1.37 to 0.72, a shift commonly interpreted as increased contribution of organic nitrates (Day et al., 2022; Farmer et al., 2010). The sustained increase in Factor 3 suggests that aqueous-phase photochemistry leads to the formation of a highly functionalized, low-volatility organic fraction that may be a significant contributor to SOA-like material in ambient fog or cloud water.

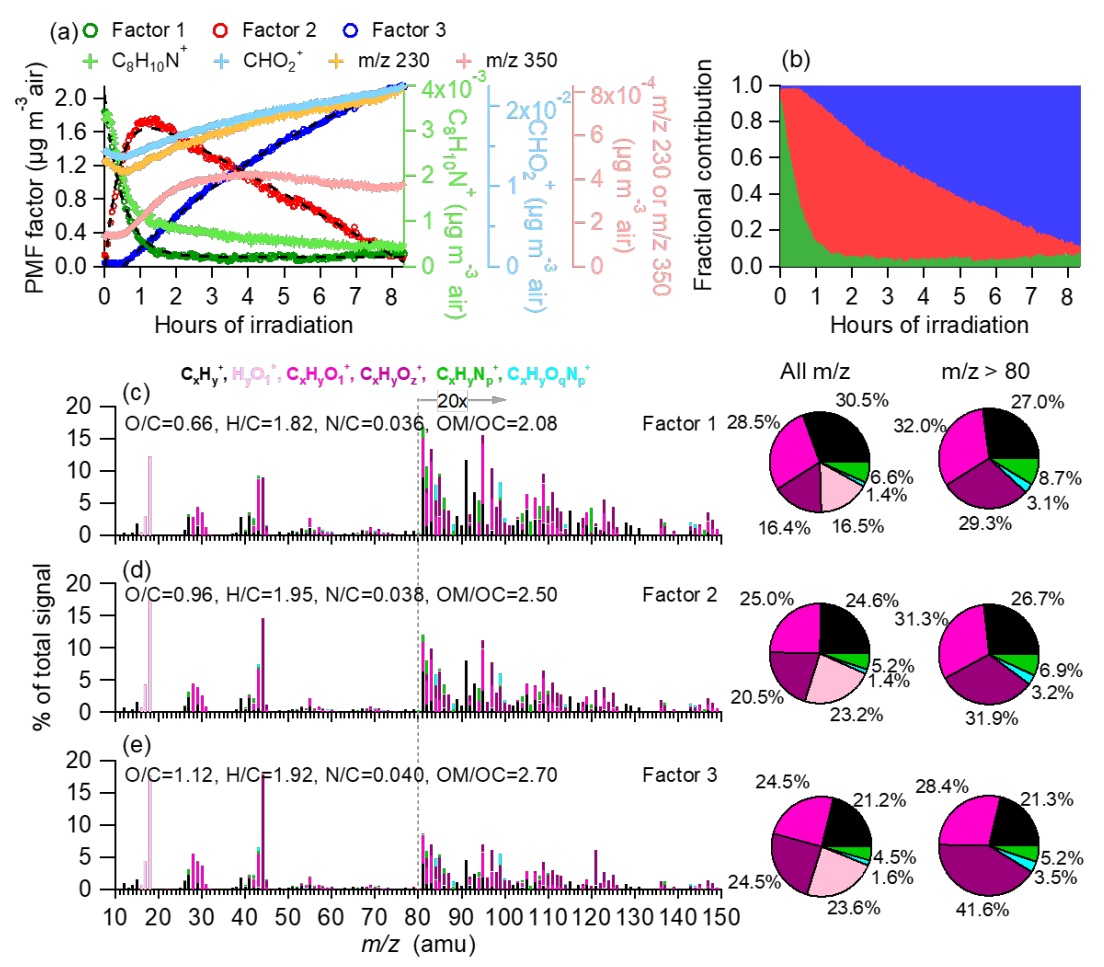


Figure 5. (a) Time series of the three-factor PMF solutions as well as tracer ions (e.g., C₈H₁₀N⁺, CHO₂⁺, m/z 230, and m/z 350) representative of the three PMF factors. Factor 1 is fitted with a three-parameter single exponential function: DOM_{OA-Fac1}=0.11+1.9e⁻

^{2.0t}. Factor 2 is fitted with a five-parameter double exponential function: DOM_{OA-Fac2}=15.6-2.1e^{-2.6t}-13.6e^{0.016t}. Factor 3 is fitted with a three-parameter single exponential function: DOM_{OA-Fac3}=3.3-3.6e^{-0.13t}. (b) Fractional contributions of the three PMF factors over time. (c–e) HR-AMS spectra of Factor 1, Factor 2, and Factor 3, respectively, with ion signals color-coded by six categories: $C_xH_y^+$, $H_yO_1^+$, $C_xH_yO_2^+$, $C_xH_yO_2^+$, $C_xH_yO_q^+$, and $C_xH_yO_qN_p^+$. Ion signals at $m/z \ge 80$ are enhanced by a factor of 20 for clarity. Calculated atomic ratios are shown in the legends. The pie charts show the relative contributions of different ion categories to each factor.

3.4 Photoinduced changes in light absorption and volatility of fog DOM

320

325

335

The optical properties of DOM in atmospheric waters have received increasing attention due to their contribution to brown carbon and their influence on Earth's radiative balance through solar absorption (Shapiro et al. 2009). To examine how fog water DOM evolves under photochemical processing, we measured its UV–visible absorbance at defined time intervals throughout the experiment. As shown in Fig. 6a, the initial fog water DOM exhibited strong absorbance in both the UV and visible regions, particularly between 300 and 500 nm relevant to tropospheric solar radiation. This absorption is attributed to conjugated chromophores, including HMW aromatic and polymeric compounds.

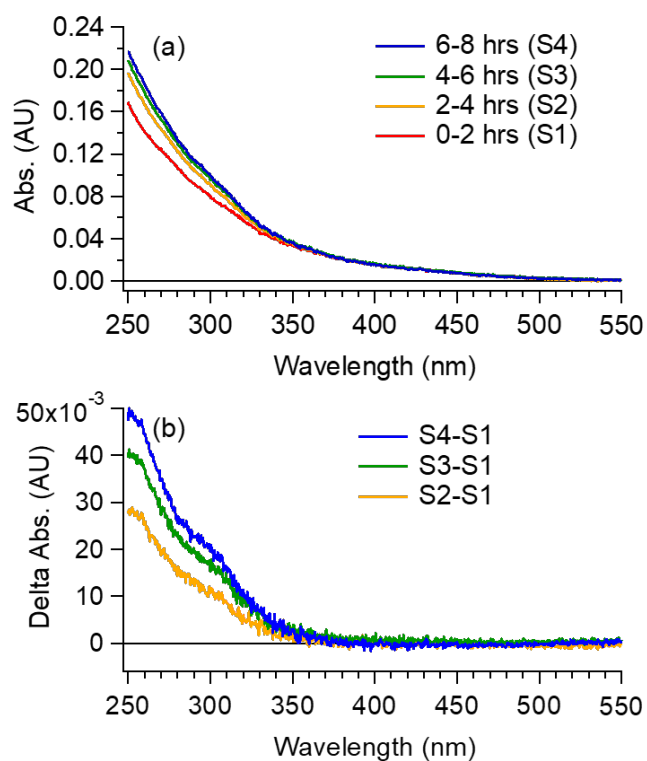


Figure 6. Evolution of UV-visible absorption of fog water sample during simulated sunlight exposure. (a) UV-visible absorbance spectra of fog water samples collected at successive illumination intervals: S1 (0-2 h), S2 (2-4 h), S3 (4-6 h) and S4 (6-8 h). (b) Differential absorbance spectra of samples S2-S4 relative to the initial sample S1.

Despite substantial chemical transformation of the DOM (e.g., increased oxidation, nitrogen incorporation, molecular fragmentation, and polymerization), the overall UV-vis spectrum revealed only modest changes over the 8-hour irradiation period. Differential absorbance spectra (relative to the initial sample, S1; Fig. 6b) revealed a slight increase in the 280–350 nm range, suggesting the formation of new light-absorbing chromophores during photochemical aging. These results indicate that

aqueous-phase oxidation can sustain, and in some cases regenerate, the light-absorbing functionality of fog water DOM. This is consistent with AMS and ESI-MS observations of CHON species formation, which likely include chromophores such as nitroaromatics and imidazoles. Although photobleaching of brown carbon chromophores is frequently assumed and has been widely observed during atmospheric aging (Hems and Abbatt, 2018; Laskin et al., 2015; Leresche et al., 2021), both laboratory and field studies have shown that aging can also enhance light absorption through the formation of new chromophores (Bianco et al., 2020; Hems et al., 2021; Laskin et al., 2025; Wu et al., 2024). Consistent with these observations, our experiments indicate that brown carbon-like optical properties can persist or even intensify during aqueous-phase processing. In particular, we observed evidence of oligomer formation, which likely contributes to the generation of new light-absorbing species. These processes have important implications for the radiative forcing potential of aged OA.

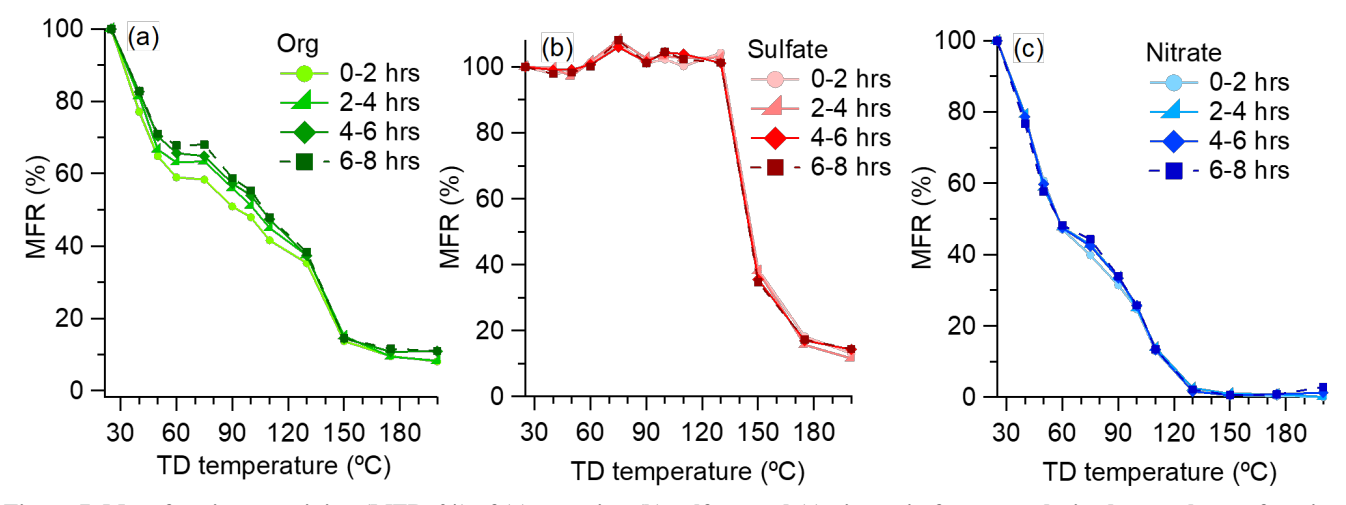


Figure 7. Mass fraction remaining (MFR, %) of (a) organics, (b) sulfate, and (c) nitrate in fog water-derived aerosols as a function of thermodenuder temperature. Each panel displays MFR trends across four irradiation periods (0-2, 2-4, 4-6, and 6-8 hours of simulated sunlight illumination).

To measure volatilities of fog-derived aerosols, we analyzed samples using HR-AMS downstream of a digitally controlled thermodenuder (TD (Fierz, Vernooij, and Burtscher 2007)), which included a bypass line and a heated line ending in an activated carbon cloth section. The TD cycled through seven set temperatures (25, 40, 65, 85, 100, 150, and 200 °C) hourly, with an automated three-way valve switching between bypass and heated modes every 5 minutes. Comparing AMS signals between these modes allowed us to assess the volatility profiles of fog water-derived aerosols. Figure 7 shows the mass fraction remaining (MFR) of organic materials (DOM_{OA}), sulfate, and nitrate as a function of thermodenuder temperature over different irradiation periods. While sulfate (Fig. 7b) and nitrate (Fig. 7c) displayed consistent volatility profiles throughout the experiment, DOM_{OA} (Fig. 7a) exhibited a clear evolution over time. Specifically, the MFR curves became progressively less steep with increased irradiation, indicating the net formation of less volatile organic species. This trend is consistent with our chemical analyses results, which show increased formation of multifunctional products and oligomers. The accumulation of highly functionalized, low-volatility compounds through aqueous-phase photochemical reactions may significantly impact the atmospheric lifetime and climate-relevant properties of OA.

4. Conclusions and atmospheric implications

365

370

375

380

385

390

This study examined the photochemical transformation of low-volatility DOM in fog water under simulated sunlight, equivalent to ~ 56 hours of wintertime tropospheric aging. The mass concentration of fog-derived DOM_{OA} increased steadily during illumination, largely due to functionalization reactions that incorporated O- and N-containing groups. Despite evidence of molecular fragmentation, total carbon mass remained largely stable, suggesting limited formation of volatile organics during aqueous-phase aging.

Both HR-AMS and positive-mode ESI-MS revealed increases in N-containing species following irradiation, along with the photooxidative transformation of CHN compounds into more oxygenated CHON and CHONS species. PMF analysis of the HR-AMS spectra resolved three distinct aging stages: unprocessed DOM_{OA} (Factor 1; O/C = 0.66, H/C = 1.82, N/C = 0.036), more oxidized intermediates (Factor 2; O/C = 0.96, H/C = 1.95, N/C = 0.038), and highly oxidized products (Factor 3; O/C = 1.12, H/C = 1.92, N/C = 0.040), with increasing O/C and N/C ratios across the factors. The accumulation of Factor 3 highlights fog processing as a source of O- and N-rich OA, potentially influencing aerosol hygroscopicity, light absorption, and toxicity. Supporting UV-vis and thermodenuder measurements confirmed that DOM_{OA} became increasingly more light-absorbing and less volatile with irradiation, consistent with the formation of highly functionalized, low-volatility species. Our findings are consistent with recent field observations in the Po Valley, Italy (Mattsson et al., 2025), which reported ON enhancement in fog water and fog residuals and attributed it to aqueous-phase formation of imidazoles. Although the Po Valley site is rural and our Fresno site is urban, both represent winter basin environments characterized by abundant liquid water and elevated nitrogen levels that favor aqueous processing and promote ON formation. The agreement between the Po Valley field observations and our laboratory aging experiments of Fresno fog DOM indicates that aqueous ON chemistry in fog is a broadly relevant pathway that may operate in diverse regions, with its magnitude influenced by local meteorology and emission sources. Overall, these results demonstrate that fog droplets act as chemically active microreactors, transforming dissolved organic matter into more oxidized, more light-absorbing and less volatile OA species during photochemical aging, beyond simply serving as scavengers of atmospheric pollutants (Collett et al. 2001, 2008; Kuang et al. 2020). Extensive laboratory and field studies have shown that oligomerization, acid formation, and imidazole formation proceed efficiently in the aqueous phase, producing agSOA and brown carbon chromophores that can modify aerosol composition, light absorption, and hygroscopicity (Faust et al. 2017; Herrmann et al. 2015; Kuang et al. 2020; McNeill 2015). Our results are consistent with prior findings and provide additional evidence for the influence of fog-driven aqueous processing on OA composition, ON speciation, volatility and light absorption. Given the frequent occurrence of winter fog and biomass burning in regions like California's San Joaquin Valley, fog-driven aqueous-phase processing likely plays a key role in regulating the atmospheric fate and climate-relevant properties of organic carbon and nitrogen. Although this study focuses on fog chemistry, similar processes are likely to occur in cloud water, with important implications for aerosol-cloud interactions and the oxidative evolution of atmospheric organic matter.

Code/Data Availability

395 All data and code used in the study are available from the corresponding author upon request.

Author contribution

LY, HK and YS collected fog samples and conducted experiments. WJ, LL, and LY analyzed the data. WJ, LY, and QZ wrote the manuscripts with input from all authors. QZ guided the research, managed the project, and defined the overarching strategy.

Competing interests

400 The authors declare that they have no conflict of interest.

Acknowledgement

This research was supported by the U.S. Department of Energy (DOE) Office of Science, Office of Biological and Environmental Research (BER), through the Atmospheric System Research (ASR) program (DE-SC00221400), the U.S. National Institute of Environmental Health Sciences Core Center (Grant P30 ES023513), and the California Agricultural Experiment Station (Projects CA-D*-ETX-2102-H). Additional support for Wenqing Jiang and Lu Yu was provided by the Jastro-Shields Graduate Research Award and the Donald G. Crosby Graduate Fellowship at UC Davis. We thank Prof. Pierre Herckes (ASU) for assisting with the Fresno fog sample collection.

Reference

- Aiken, Allison C., Peter F. DeCarlo, Jesse H. Kroll, Douglas R. Worsnop, J. Alex Huffman, Kenneth S. Docherty, Ingrid M.
 Ulbrich, Claudia Mohr, Joel R. Kimmel, Donna Sueper, Yele Sun, Qi Zhang, Achim Trimborn, Megan Northway, Paul J. Ziemann, Manjula R. Canagaratna, Timothy B. Onasch, M. Rami Alfarra, Andre S. H. Prevot, Josef Dommen, Jonathan Duplissy, Axel Metzger, Urs Baltensperger, and Jose L. Jimenez. 2008. "O/C and OM/OC Ratios of Primary, Secondary, and Ambient Organic Aerosols with High-Resolution Time-of-Flight Aerosol Mass Spectrometry." Environmental Science & Technology 42(12):4478–85. doi: 10.1021/es703009q.
- Allan, James D., Keith N. Bower, Hugh Coe, Hacene Boudries, John T. Jayne, Manjula R. Canagaratna, Dylan B. Millet, Allen H. Goldstein, Patricia K. Quinn, Rodney J. Weber, and Douglas R. Worsnop. 2004. "Submicron Aerosol Composition at Trinidad Head, California, during ITCT 2K2: Its Relationship with Gas Phase Volatile Organic Carbon and Assessment of Instrument Performance." *Journal of Geophysical Research: Atmospheres* 109(D23). doi: https://doi.org/10.1029/2003JD004208.

Altieri, K E, B. J. Turpin, and S. P. Seitzinger. 2009. "Oligomers, Organosulfates, and Nitrooxy Organosulfates in Rainwater Identified by Ultra-High Resolution Electrospray Ionization FT-ICR Mass Spectrometry." *Atmos. Chem. Phys.* 9(7):2533–42. doi: 10.5194/acp-9-2533-2009.

425

435

- Altieri, Katye E, Barbara J. Turpin, and Sybil P. Seitzinger. 2009. "Composition of Dissolved Organic Nitrogen in Continental Precipitation Investigated by Ultra-High Resolution FT-ICR Mass Spectrometry." *Environmental Science & Technology* 43(18):6950–55. doi: 10.1021/es9007849.
- Anastasio, Cort, Bruce C. Faust, and C. Janakiram Rao. 1997. "Aromatic Carbonyl Compounds as Aqueous-Phase Photochemical Sources of Hydrogen Peroxide in Acidic Sulfate Aerosols, Fogs, and Clouds. 1. Non-Phenolic Methoxybenzaldehydes and Methoxyacetophenones with Reductants (Phenols)." *Environmental Science & Technology* 31(1):218–32. doi: 10.1021/es960359g.
- Anastasio, Cort, and Keith G. McGregor. 2001. "Chemistry of Fog Waters in California's Central Valley: 1. In Situ Photoformation of Hydroxyl Radical and Singlet Molecular Oxygen." *Atmospheric Environment* 35(6):1079–89. doi: https://doi.org/10.1016/S1352-2310(00)00281-8.
 - Arciva, Stephanie, Christopher Niedek, Camille Mavis, Melanie Yoon, Martin Esparza Sanchez, Qi Zhang, and Cort Anastasio. 2022. "Aqueous ·OH Oxidation of Highly Substituted Phenols as a Source of Secondary Organic Aerosol." Environmental Science & Technology 56(14):9959–67. doi: 10.1021/acs.est.2c02225.
 - Bianco, Angelica, Laurent Deguillaume, Mickaël Vaïtilingom, Edith Nicol, Jean-Luc Baray, Nadine Chaumerliac, and Maxime Bridoux. 2018. "Molecular Characterization of Cloud Water Samples Collected at the Puy de Dôme (France) by Fourier Transform Ion Cyclotron Resonance Mass Spectrometry." *Environmental Science & Technology* 52(18):10275–85. doi: 10.1021/acs.est.8b01964.
- 440 Bianco, Angelica, Monica Passananti, Marcello Brigante, and Gilles Mailhot. 2020. "Photochemistry of the Cloud Aqueous Phase: A Review." *Molecules* 25(2).
 - Borduas-Dedekind, N., R. Ossola, R. O. David, L. S. Boynton, V. Weichlinger, Z. A. Kanji, and K. McNeill. 2019. "Photomineralization Mechanism Changes the Ability of Dissolved Organic Matter to Activate Cloud Droplets and to Nucleate Ice Crystals." *Atmos. Chem. Phys.* 19(19):12397–412. doi: 10.5194/acp-19-12397-2019.
- 445 Boris, Alexandra J., Denise C. Napolitano, Pierre Herckes, Andrea L. Clements, and Jr. Collett Jeffrey L. 2018. "Fogs and Air Quality on the Southern California Coast." Aerosol and Air Quality Research 18(1):224–39. doi: 10.4209/aaqr.2016.11.0522.
 - Brege, M., M. Paglione, S. Gilardoni, S. Decesari, M. C. Facchini, and L. R. Mazzoleni. 2018. "Molecular Insights on Aging and Aqueous-Phase Processing from Ambient Biomass Burning Emissions-Influenced Po Valley Fog and Aerosol." *Atmos. Chem. Phys.* 18(17):13197–214. doi: 10.5194/acp-18-13197-2018.
 - Brezonik, Patrick L., and Jennifer Fulkerson-Brekken. 1998. "Nitrate-Induced Photolysis in Natural Waters: Controls on Concentrations of Hydroxyl Radical Photo-Intermediates by Natural Scavenging Agents." *Environmental Science & Technology* 32(19):3004–10. doi: 10.1021/es9802908.

- Canagaratna, M. R., J. L. Jimenez, J. H. Kroll, Q. Chen, S. H. Kessler, P. Massoli, L. Hildebrandt Ruiz, E. Fortner, L. R.
 Williams, K. R. Wilson, J. D. Surratt, N. M. Donahue, J. T. Jayne, and D. R. Worsnop. 2015. "Elemental Ratio Measurements of Organic Compounds Using Aerosol Mass Spectrometry: Characterization, Improved Calibration, and Implications." *Atmos. Chem. Phys.* 15(1):253–72. doi: 10.5194/acp-15-253-2015.
 - Chen, Chia-Li, Sijie Chen, Lynn M. Russell, Jun Liu, Derek J. Price, Raghu Betha, Kevin J. Sanchez, Alex K. Y. Lee, Leah Williams, Sonya C. Collier, Qi Zhang, Anikender Kumar, Michael J. Kleeman, Xiaolu Zhang, and Christopher D. Cappa. 2018. "Organic Aerosol Particle Chemical Properties Associated With Residential Burning and Fog in Wintertime San Joaquin Valley (Fresno) and With Vehicle and Firework Emissions in Summertime South Coast Air Basin (Fontana)."

 Journal of Geophysical Research: Atmospheres 123(18):10,707-710,731. doi: 10.1029/2018JD028374.

- Collett, Jeffrey L., Pierre Herckes, Sarah Youngster, and Taehyoung Lee. 2008. "Processing of Atmospheric Organic Matter by California Radiation Fogs." *Atmospheric Research* 87(3):232–41. doi: https://doi.org/10.1016/j.atmosres.2007.11.005.
- Collett, Jeffrey L., D. Eli Sherman, Katharine F. Moore, Michael P. Hannigan, and Taehyoung Lee. 2001. "Aerosol Particle Processing and Removal by Fogs: Observations in Chemically Heterogeneous Central California Radiation Fogs." *Water, Air and Soil Pollution: Focus* 1(5):303–12. doi: 10.1023/A:1013175709931.
- Collier, Sonya, Leah R. Williams, Timothy B. Onasch, Christopher D. Cappa, Xiaolu Zhang, Lynn M. Russell, Chia-Li Chen,
 Kevin J. Sanchez, Douglas R. Worsnop, and Qi Zhang. 2018. "Influence of Emissions and Aqueous Processing on
 Particles Containing Black Carbon in a Polluted Urban Environment: Insights From a Soot Particle-Aerosol Mass
 Spectrometer." *Journal of Geophysical Research: Atmospheres* 123(12):6648–66. doi: https://doi.org/10.1002/2017JD027851.
- Day, D. A., P. Campuzano-Jost, B. A. Nault, B. B. Palm, W. Hu, H. Guo, P. J. Wooldridge, R. C. Cohen, K. S. Docherty, J.
 A. Huffman, S. S. de Sá, S. T. Martin, and J. L. Jimenez. 2022. "A Systematic Re-Evaluation of Methods for Quantification of Bulk Particle-Phase Organic Nitrates Using Real-Time Aerosol Mass Spectrometry." *Atmos. Meas. Tech.* 15(2):459–83. doi: 10.5194/amt-15-459-2022.
- DeCarlo, Peter F., Joel R. Kimmel, Achim Trimborn, Megan J. Northway, John T. Jayne, Allison C. Aiken, Marc Gonin, Katrin Fuhrer, Thomas Horvath, Kenneth S. Docherty, Doug R. Worsnop, and Jose L. Jimenez. 2006. "Field-Deployable, High-Resolution, Time-of-Flight Aerosol Mass Spectrometer." *Analytical Chemistry* 78(24):8281–89. doi: 10.1021/ac061249n.
 - Demoz, B. B., J. L. Collett, and B. C. Daube. 1996. "On the Caltech Active Strand Cloudwater Collectors." *Atmospheric Research* 41(1):47–62. doi: https://doi.org/10.1016/0169-8095(95)00044-5.
- Desyaterik, Yury, Yele Sun, Xinhua Shen, Taehyoung Lee, Xinfeng Wang, Tao Wang, and Jeffrey L. Collett Jr. 2013. "Speciation of 'Brown' Carbon in Cloud Water Impacted by Agricultural Biomass Burning in Eastern China." *Journal of Geophysical Research: Atmospheres* 118(13):7389–99. doi: https://doi.org/10.1002/jgrd.50561.
 - Ehrenhauser, Franz S., Kalindi Khadapkar, Youliang Wang, James W. Hutchings, Olivier Delhomme, Raghava R.

- Kommalapati, Pierre Herckes, Mary J. Wornat, and Kalliat T. Valsaraj. 2012. "Processing of Atmospheric Polycyclic Aromatic Hydrocarbons by Fog in an Urban Environment." *Journal of Environmental Monitoring* 14(10):2566–79. doi: 10.1039/C2EM30336A.
- Ervens, Barbara, Annmarie G. Carlton, Barbara J. Turpin, Katye E. Altieri, Sonia M. Kreidenweis, and Graham Feingold. 2008. "Secondary Organic Aerosol Yields from Cloud-Processing of Isoprene Oxidation Products." *Geophysical Research Letters* 35(2). doi: https://doi.org/10.1029/2007GL031828.
- Farley, Ryan N., Sonya Collier, Christopher D. Cappa, Leah R. Williams, Timothy B. Onasch, Lynn M. Russell, Hwajin Kim, and Qi Zhang. 2023. "Source Apportionment of Soot Particles and Aqueous-Phase Processing of Black Carbon Coatings in an Urban Environment." *Atmospheric Chemistry and Physics* 23(23):15039–56. doi: 10.5194/acp-23-15039-2023.

500

505

- Farmer, D. K., A. Matsunaga, K. S. Docherty, J. D. Surratt, J. H. Seinfeld, P. J. Ziemann, and J. L. Jimenez. 2010. "Response of an Aerosol Mass Spectrometer to Organonitrates and Organosulfates and Implications for Atmospheric Chemistry." *Proceedings of the National Academy of Sciences of the United States of America* 107(15):6670–75. doi: 10.1073/pnas.0912340107.
- Faust, Jennifer A., Jenny P. S. Wong, Alex K. Y. Lee, and Jonathan P. D. Abbatt. 2017. "Role of Aerosol Liquid Water in Secondary Organic Aerosol Formation from Volatile Organic Compounds." *Environmental Science & Technology* 51(3):1405–13. doi: 10.1021/acs.est.6b04700.
- Fierz, Martin, Martine G. C. Vernooij, and Heinz Burtscher. 2007. "An Improved Low-Flow Thermodenuder." *Journal of Aerosol Science* 38(11):1163–68. doi: https://doi.org/10.1016/j.jaerosci.2007.08.006.
 - Ge, Xinlei, Ari Setyan, Yele Sun, and Qi Zhang. 2012. "Primary and Secondary Organic Aerosols in Fresno, California during Wintertime: Results from High Resolution Aerosol Mass Spectrometry." *Journal of Geophysical Research: Atmospheres* 117(D19). doi: 10.1029/2012JD018026.
- Ge, Xinlei, Qi Zhang, Yele Sun, Christopher R. Ruehl, and Ari Setyan. 2012. "Effect of Aqueous-Phase Processing on Aerosol Chemistry and Size Distributions in Fresno, California, during Wintertime." *Environmental Chemistry* 9(3):221–35.
- George, Kathryn M., Travis C. Ruthenburg, Jeremy Smith, Lu Yu, Qi Zhang, Cort Anastasio, and Ann M. Dillner. 2015. "FT-IR Quantification of the Carbonyl Functional Group in Aqueous-Phase Secondary Organic Aerosol from Phenols." *Atmospheric Environment* 100:230–37. doi: 10.1016/j.atmosenv.2014.11.011.
- Gilardoni, Stefania, Paola Massoli, Marco Paglione, Lara Giulianelli, Claudio Carbone, Matteo Rinaldi, Stefano Decesari, Silvia Sandrini, Francesca Costabile, Gian Paolo Gobbi, Maria Chiara Pietrogrande, Marco Visentin, Fabiana Scotto, Sandro Fuzzi, Maria Cristina Facchini, Gilardoni Stefania, Massoli Paola, Paglione Marco, Giulianelli Lara, Carbone Claudio, Rinaldi Matteo, Decesari Stefano, Sandrini Silvia, Costabile Francesca, Gobbi Gian Paolo, Pietrogrande Maria Chiara, Visentin Marco, Scotto Fabiana, Fuzzi Sandro, and Facchini Maria Cristina. 2016. "Direct Observation of Aqueous Secondary Organic Aerosol from Biomass-Burning Emissions." *Proceedings of the National Academy of Sciences* 113(36):10013–18. doi: 10.1073/pnas.1602212113.
 - Haan, David O. De, Ashley L. Corrigan, Kyle W. Smith, Daniel R. Stroik, Jacob J. Turley, Frances E. Lee, Margaret A.

- Tolbert, Jose L. Jimenez, Kyle E. Cordova, and Grant R. Ferrell. 2009. "Secondary Organic Aerosol-Forming Reactions of Glyoxal with Amino Acids." *Environmental Science & Technology* 43(8):2818–24. doi: 10.1021/es803534f.
- Hawkins, Lelia N., Amanda N. Lemire, Melissa M. Galloway, Ashley L. Corrigan, Jacob J. Turley, Brenna M. Espelien, and David O. De Haan. 2016. "Maillard Chemistry in Clouds and Aqueous Aerosol As a Source of Atmospheric Humic-Like Substances." *Environmental Science & Technology* 50(14):7443–52. doi: 10.1021/acs.est.6b00909.
 - Hems, Rachel F., and Jonathan P. D. Abbatt. 2018. "Aqueous Phase Photo-Oxidation of Brown Carbon Nitrophenols: Reaction Kinetics, Mechanism, and Evolution of Light Absorption." *ACS Earth and Space Chemistry* 2(3):225–34. doi: 10.1021/acsearthspacechem.7b00123.
- Hems, Rachel F., Elijah G. Schnitzler, Monica Bastawrous, Ronald Soong, André J. Simpson, and Jonathan P. D. Abbatt. 2020. "Aqueous Photoreactions of Wood Smoke Brown Carbon." *ACS Earth and Space Chemistry* 4(7):1149–60. doi: 10.1021/acsearthspacechem.0c00117.

540

- Hems, Rachel F., Elijah G. Schnitzler, Carolyn Liu-Kang, Christopher D. Cappa, and Jonathan P. D. Abbatt. 2021. "Aging of Atmospheric Brown Carbon Aerosol." *ACS Earth and Space Chemistry* 5(4):722–48. doi: 10.1021/acsearthspacechem.0c00346.
- Herckes, P., A. R. Marcotte, Y. Wang, and J. L. Collett. 2015. "Fog Composition in the Central Valley of California over Three Decades." *Atmospheric Research* 151:20–30. doi: https://doi.org/10.1016/j.atmosres.2014.01.025.
- Herckes, Pierre, Michael P. Hannigan, Laurie Trenary, Taehyoung Lee, and Jeffrey L. Collett. 2002. "Organic Compounds in Radiation Fogs in Davis (California)." *Atmospheric Research* 64(1):99–108. doi: https://doi.org/10.1016/S0169-8095(02)00083-2.
- Herckes, Pierre, Taehyoung Lee, Laurie Trenary, Gongunn Kang, Hui Chang, and Jeffrey L. Collett. 2002. "Organic Matter in Central California Radiation Fogs." *Environmental Science & Technology* 36(22):4777–82. doi: 10.1021/es025889t.
- Herckes, Pierre, Jerry A. Leenheer, and Jeffrey L. Collett. 2007. "Comprehensive Characterization of Atmospheric Organic Matter in Fresno, California Fog Water." *Environmental Science & Technology* 41(2):393–99. doi: 10.1021/es0607988.
- Herckes, Pierre, Kalliat T. Valsaraj, and Jeffrey L. Collett. 2013. "A Review of Observations of Organic Matter in Fogs and Clouds: Origin, Processing and Fate." *Atmospheric Research* 132–133:434–49. doi: https://doi.org/10.1016/j.atmosres.2013.06.005.
 - Herrmann, Hartmut, Thomas Schaefer, Andreas Tilgner, Sarah A. Styler, Christian Weller, Monique Teich, and Tobias Otto. 2015. "Tropospheric Aqueous-Phase Chemistry: Kinetics, Mechanisms, and Its Coupling to a Changing Gas Phase." *Chemical Reviews* 115(10):4259–4334. doi: 10.1021/cr500447k.
 - Huang, Dan Dan, Qi Zhang, Heidi H. Y. Cheung, Lu Yu, Shan Zhou, Cort Anastasio, Jeremy D. Smith, and Chak K. Chan. 2018. "Formation and Evolution of AqSOA from Aqueous-Phase Reactions of Phenolic Carbonyls: Comparison between Ammonium Sulfate and Ammonium Nitrate Solutions." *Environmental Science and Technology* 52(16):9215– 24. doi: 10.1021/acs.est.8b03441.
- 555 Jiang, Wenging, Maria V Misovich, Anusha P. S. Hettiyadura, Alexander Laskin, Alexander S. McFall, Cort Anastasio, and

- Qi Zhang. 2021. "Photosensitized Reactions of a Phenolic Carbonyl from Wood Combustion in the Aqueous Phase—Chemical Evolution and Light Absorption Properties of AqSOA." *Environmental Science & Technology* 55(8):5199–5211. doi: 10.1021/acs.est.0c07581.
- Jiang, Wenqing, Christopher Niedek, Cort Anastasio, and Qi Zhang. 2023. "Photoaging of Phenolic Secondary Organic Aerosol in the Aqueous Phase: Evolution of Chemical and Optical Properties and Effects of Oxidants." *Atmospheric Chemistry and Physics* 23(12):7103–20. doi: 10.5194/acp-23-7103-2023.
 - Kaur, R., and C. Anastasio. 2017. "Light Absorption and the Photoformation of Hydroxyl Radical and Singlet Oxygen in Fog Waters." *Atmospheric Environment* 164:387–97. doi: https://doi.org/10.1016/j.atmosenv.2017.06.006.
 - Kaur, R., B. M. Hudson, J. Draper, D. J. Tantillo, and C. Anastasio. 2019. "Aqueous Reactions of Organic Triplet Excited States with Atmospheric Alkenes." *Atmos. Chem. Phys.* 19(7):5021–32. doi: 10.5194/acp-19-5021-2019.

- Kim, Hwajin, Sonya Collier, Xinlei Ge, Jianzhong Xu, Yele Sun, Wenqing Jiang, Youliang Wang, Pierre Herckes, and Qi Zhang. 2019. "Chemical Processing of Water-Soluble Species and Formation of Secondary Organic Aerosol in Fogs."

 Atmospheric Environment 200:158–66. doi: https://doi.org/10.1016/j.atmosenv.2018.11.062.
- Kuang, Ye, Yao He, Wanyun Xu, Bin Yuan, Gen Zhang, Zhiqiang Ma, Caihong Wu, Chaomin Wang, Sihang Wang, Shenyang Zhang, Jiangchuan Tao, Nan Ma, Hang Su, Yafang Cheng, Min Shao, and Yele Sun. 2020. "Photochemical Aqueous-Phase Reactions Induce Rapid Daytime Formation of Oxygenated Organic Aerosol on the North China Plain."

 Environmental Science & Technology 54(7):3849–60. doi: 10.1021/acs.est.9b06836.
 - Laskin, Alexander, Julia Laskin, and Sergey A. Nizkorodov. 2015. "Chemistry of Atmospheric Brown Carbon." *Chemical Reviews* 115(10):4335–82. doi: 10.1021/cr5006167.
- 575 Laskin, Alexander, Christopher P. West, and Anusha P. S. Hettiyadura. 2025. "Molecular Insights into the Composition, Sources, and Aging of Atmospheric Brown Carbon." *Chemical Society Reviews* 54(3):1583–1612. doi: 10.1039/D3CS00609C.
 - Lee, A. K. Y., K. L. Hayden, P. Herckes, W. R. Leaitch, J. Liggio, A. M. Macdonald, and J. P. D. Abbatt. 2012. "Characterization of Aerosol and Cloud Water at a Mountain Site during WACS 2010: Secondary Organic Aerosol Formation through Oxidative Cloud Processing." *Atmos. Chem. Phys.* 12(15):7103–16. doi: 10.5194/acp-12-7103-2012.
 - Leresche, Frank, Joseph R. Salazar, David J. Pfotenhauer, Michael P. Hannigan, Brian J. Majestic, and Fernando L. Rosario-Ortiz. 2021. "Photochemical Aging of Atmospheric Particulate Matter in the Aqueous Phase." *Environmental Science and Technology* 55(19):13152–63. doi: 10.1021/acs.est.1c00978.
- Li, Yumin, Tzung-May Fu, Jian Zhen Yu, Xu Yu, Qi Chen, Ruqian Miao, Yang Zhou, Aoxing Zhang, Jianhuai Ye, Xin Yang,
 Shu Tao, Hongbin Liu, and Weiqi Yao. 2023. "Dissecting the Contributions of Organic Nitrogen Aerosols to Global
 Atmospheric Nitrogen Deposition and Implications for Ecosystems." *National Science Review* 10(12):nwad244. doi: 10.1093/nsr/nwad244.
 - Liu, Jun, Matthew J. Gunsch, Claire E. Moffett, Lu Xu, Rime El Asmar, Qi Zhang, Thomas B. Watson, Hannah M. Allen, John D. Crounse, Jason St. Clair, Michelle Kim, Paul O. Wennberg, Rodney J. Weber, Rebecca J. Sheesley, and Kerri

- A. Pratt. 2021. "Hydroxymethanesulfonate (HMS) Formation during Summertime Fog in an Arctic Oil Field." *Environmental Science & Technology Letters* 8(7):511–18. doi: 10.1021/acs.estlett.1c00357.
 - Mattsson, F., A. Neuberger, L. Heikkinen, Y. Gramlich, M. Paglione, M. Rinaldi, S. Decesari, P. Zieger, I. Riipinen, and C. Mohr. 2025. "Enrichment of Organic Nitrogen in Fog Residuals Observed in the Italian Po Valley." *Atmos. Chem. Phys.* 25(14):7973–89. doi: 10.5194/acp-25-7973-2025.
- Mazzoleni, Lynn R., Brandie M. Ehrmann, Xinhua Shen, Alan G. Marshall, and Jeffrey L. Collett. 2010. "Water-Soluble Atmospheric Organic Matter in Fog: Exact Masses and Chemical Formula Identification by Ultrahigh-Resolution Fourier Transform Ion Cyclotron Resonance Mass Spectrometry." *Environmental Science & Technology* 44(10):3690–97. doi: 10.1021/es903409k.
- McNeill, Kristopher, and Silvio Canonica. 2016. "Triplet State Dissolved Organic Matter in Aquatic Photochemistry: Reaction

 Mechanisms, Substrate Scope, and Photophysical Properties." *Environmental Science: Processes & Impacts*18(11):1381–99. doi: 10.1039/C6EM00408C.
 - McNeill, V. Faye. 2015. "Aqueous Organic Chemistry in the Atmosphere: Sources and Chemical Processing of Organic Aerosols." *Environmental Science & Technology* 49(3):1237–44. doi: 10.1021/es5043707.
- Ng, N. L., M. R. Canagaratna, J. L. Jimenez, P. S. Chhabra, J. H. Seinfeld, and D. R. Worsnop. 2011. "Changes in Organic Aerosol Composition with Aging Inferred from Aerosol Mass Spectra." *Atmos. Chem. Phys.* 11(13):6465–74. doi: 10.5194/acp-11-6465-2011.
 - Ng, N. L., M. R. Canagaratna, Q. Zhang, J. L. Jimenez, J. Tian, I. M. Ulbrich, J. H. Kroll, K. S. Docherty, P. S. Chhabra, R. Bahreini, S. M. Murphy, J. H. Seinfeld, L. Hildebrandt, N. M. Donahue, P. F. DeCarlo, V. A. Lanz, A. S. H. Prévôt, E. Dinar, Y. Rudich, and D. R. Worsnop. 2010. "Organic Aerosol Components Observed in Northern Hemispheric Datasets from Aerosol Mass Spectrometry." *Atmos. Chem. Phys.* 10(10):4625–41. doi: 10.5194/acp-10-4625-2010.

- Nozière, Barbara, Pawel Dziedzic, and Armando Córdova. 2009. "Products and Kinetics of the Liquid-Phase Reaction of Glyoxal Catalyzed by Ammonium Ions (NH4+)." *The Journal of Physical Chemistry A* 113(1):231–37. doi: 10.1021/jp8078293.
- Ossola, Rachele, Oskar Martin Jönsson, Kyle Moor, and Kristopher McNeill. 2021. "Singlet Oxygen Quantum Yields in Environmental Waters." *Chemical Reviews* 121(7):4100–4146. doi: 10.1021/acs.chemrev.0c00781.
 - Paatero, Pentti, and Unto Tapper. 1994. "Positive Matrix Factorization: A Non-Negative Factor Model with Optimal Utilization of Error Estimates of Data Values." *Environmetrics* 5(2):111–26. doi: https://doi.org/10.1002/env.3170050203.
- Pailler, L., L. Deguillaume, H. Lavanant, I. Schmitz, M. Hubert, E. Nicol, M. Ribeiro, J. M. Pichon, M. Vaïtilingom, P. Dominutti, F. Burnet, P. Tulet, M. Leriche, and A. Bianco. 2024. "Molecular Composition of Clouds: A Comparison between Samples Collected at Tropical (Réunion Island, France) and Mid-North (Puy de Dôme, France) Latitudes."

 Atmos. Chem. Phys. 24(9):5567–84. doi: 10.5194/acp-24-5567-2024.
 - Parworth, Caroline L., Dominique E. Young, Hwajin Kim, Xiaolu Zhang, Christopher D. Cappa, Sonya Collier, and Qi Zhang.

- 2017. "Wintertime Water-Soluble Aerosol Composition and Particle Water Content in Fresno, California." *Journal of Geophysical Research: Atmospheres* 122(5):3155–70. doi: 10.1002/2016JD026173.
 - Pratap, Vikram, Amy E. Christiansen, Annmarie G. Carlton, Sara Lance, Paul Casson, Jed Dukett, Hesham Hassan, James J. Schwab, and Christopher J. Hennigan. 2021. "Investigating the Evolution of Water-Soluble Organic Carbon in Evaporating Cloud Water." *Environmental Science: Atmospheres* 1(1):21–30. doi: 10.1039/D0EA00005A.
- Pratt, Kerri A., Marc N. Fiddler, Paul B. Shepson, Annmarie G. Carlton, and Jason D. Surratt. 2013. "Organosulfates in Cloud Water above the Ozarks' Isoprene Source Region." *Atmospheric Environment* 77:231–38. doi: https://doi.org/10.1016/j.atmosenv.2013.05.011.
 - Renard, P., F. Siekmann, G. Salque, C. Demelas, B. Coulomb, L. Vassalo, S. Ravier, B. Temime-Roussel, D. Voisin, and A. Monod. 2015. "Aqueous-Phase Oligomerization of Methyl Vinyl Ketone through Photooxidation Part 1: Aging Processes of Oligomers." *Atmos. Chem. Phys.* 15(1):21–35. doi: 10.5194/acp-15-21-2015.
- Roach, Patrick J., Julia Laskin, and Alexander Laskin. 2011. "Higher-Order Mass Defect Analysis for Mass Spectra of Complex Organic Mixtures." *Analytical Chemistry* 83(12):4924–29. doi: 10.1021/ac200654j.
 - Schneider, J., S. Mertes, D. van Pinxteren, H. Herrmann, and S. Borrmann. 2017. "Uptake of Nitric Acid, Ammonia, and Organics in Orographic Clouds: Mass Spectrometric Analyses of Droplet Residual and Interstitial Aerosol Particles." Atmos. Chem. Phys. 17(2):1571–93. doi: 10.5194/acp-17-1571-2017.
- 640 Schurman, Misha I., Alexandra Boris, Yury Desyaterik, and Jr. Collett Jeffrey L. 2018. "Aqueous Secondary Organic Aerosol Formation in Ambient Cloud Water Photo-Oxidations." *Aerosol and Air Quality Research* 18(1):15–25. doi: 10.4209/aaqr.2017.01.0029.

- Shapiro, E. L., J. Szprengiel, N. Sareen, C. N. Jen, M. R. Giordano, and V. F. McNeill. 2009. "Light-Absorbing Secondary Organic Material Formed by Glyoxal in Aqueous Aerosol Mimics." *Atmos. Chem. Phys.* 9(7):2289–2300. doi: 10.5194/acp-9-2289-2009.
- Smith, Jeremy D., Haley Kinney, and Cort Anastasio. 2015. "Aqueous Benzene-Diols React with an Organic Triplet Excited State and Hydroxyl Radical to Form Secondary Organic Aerosol." *Physical Chemistry Chemical Physics* 17(15):10227–37. doi: 10.1039/c4cp06095d.
- Sun, W., Y. Fu, G. Zhang, Y. Yang, F. Jiang, X. Lian, B. Jiang, Y. Liao, X. Bi, D. Chen, J. Chen, X. Wang, J. Ou, P. Peng, and G. Sheng. 2021. "Measurement Report: Molecular Characteristics of Cloud Water in Southern China and Insights into Aqueous-Phase Processes from Fourier Transform Ion Cyclotron Resonance Mass Spectrometry." *Atmos. Chem. Phys.* 21(22):16631–44. doi: 10.5194/acp-21-16631-2021.
 - Sun, Wei, Xiaodong Hu, Yuzhen Fu, Guohua Zhang, Yujiao Zhu, Xinfeng Wang, C. Yan, L. Xue, H. Meng, B. Jiang, Y. Liao, Xinfeng Wang, P. Peng, and X. Bi. 2024. "Different Formation Pathways of Nitrogen-Containing Organic Compounds in Aerosols and Fog Water in Northern China." *EGUsphere* 2024(February):1–22. doi: 10.5194/egusphere-2024-74.
 - Sun, Y. L., Q. Zhang, C. Anastasio, and J. Sun. 2010. "Insights into Secondary Organic Aerosol Formed via Aqueous-Phase Reactions of Phenolic Compounds Based on High Resolution Mass Spectrometry." Atmos. Chem. Phys. 10(10):4809—

22. doi: 10.5194/acp-10-4809-2010.

- Tomaz, Sophie, Tianqu Cui, Yuzhi Chen, Kenneth G. Sexton, James M. Roberts, Carsten Warneke, Robert J. Yokelson, Jason
 D. Surratt, and Barbara J. Turpin. 2018. "Photochemical Cloud Processing of Primary Wildfire Emissions as a Potential
 Source of Secondary Organic Aerosol." *Environmental Science & Technology* 52(19):11027–37. doi: 10.1021/acs.est.8b03293.
 - Ulbrich, I. M., M. R. Canagaratna, Q. Zhang, D. R. Worsnop, and J. L. Jimenez. 2009. "Interpretation of Organic Components from Positive Matrix Factorization of Aerosol Mass Spectrometric Data." *Atmospheric Chemistry and Physics* 9(9):2891–2918. doi: 10.5194/acp-9-2891-2009.
 - Wang, Junfeng, Jianhuai Ye, Qi Zhang, Jian Zhao, Yangzhou Wu, Jingyi Li, Dantong Liu, Weijun Li, Yange Zhang, Cheng Wu, Conghui Xie, Yiming Qin, Yali Lei, Xiangpeng Huang, Jianping Guo, Pengfei Liu, Pingqing Fu, Yongjie Li, Hyun Chul Lee, Hyoungwoo Choi, Jie Zhang, Hong Liao, Mindong Chen, Yele Sun, Xinlei Ge, Scot T. Martin, and Daniel J. Jacob. 2021. "Aqueous Production of Secondary Organic Aerosol from Fossil-Fuel Emissions in Winter Beijing Haze."
- Proceedings of the National Academy of Sciences of the United States of America 118(8):1–6. doi: 10.1073/pnas.2022179118.
 - Wang, Youliang, Chao-An Chiu, Paul Westerhoff, Kalliat T. Valsaraj, and Pierre Herckes. 2013. "Characterization of Atmospheric Organic Matter Using Size-Exclusion Chromatography with Inline Organic Carbon Detection." *Atmospheric Environment* 68:326–32. doi: https://doi.org/10.1016/j.atmosenv.2012.11.049.
- Wu, Yangzhou, Quan Liu, Dantong Liu, Ping Tian, Weiqi Xu, Junfeng Wang, Kang Hu, Siyuan Li, Xiaotong Jiang, Fei Wang, Mengyu Huang, Deping Ding, Chenjie Yu, and Dawei Hu. 2024. "Enhanced Formation of Nitrogenous Organic Aerosols and Brown Carbon after Aging in the Planetary Boundary Layer." Npj Climate and Atmospheric Science 7(1):179. doi: 10.1038/s41612-024-00726-x.
- Youn, J. S., E. Crosbie, L. C. Maudlin, Z. Wang, and A. Sorooshian. 2015. "Dimethylamine as a Major Alkyl Amine Species in Particles and Cloud Water: Observations in Semi-Arid and Coastal Regions." *Atmospheric Environment* 122:250–58. doi: https://doi.org/10.1016/j.atmosenv.2015.09.061.
 - Young, D. E., H. Kim, C. Parworth, S. Zhou, X. Zhang, C. D. Cappa, R. Seco, S. Kim, and Q. Zhang. 2016. "Influences of Emission Sources and Meteorology on Aerosol Chemistry in a Polluted Urban Environment: Results from DISCOVER-AQ California." Atmos. Chem. Phys. 16(8):5427–51. doi: 10.5194/acp-16-5427-2016.
- Yu, L., J. Smith, A. Laskin, C. Anastasio, J. Laskin, and Q. Zhang. 2014. "Chemical Characterization of SOA Formed from Aqueous-Phase Reactions of Phenols with the Triplet Excited State of Carbonyl and Hydroxyl Radical." Atmospheric Chemistry and Physics 14(24):13801–16. doi: 10.5194/acp-14-13801-2014.
- Yu, L., J. Smith, A. Laskin, K. M. George, C. Anastasio, J. Laskin, A. M. Dillner, and Q. Zhang. 2016. "Molecular Transformations of Phenolic SOA during Photochemical Aging in the Aqueous Phase: Competition among Oligomerization, Functionalization, and Fragmentation." *Atmos. Chem. Phys.* 16(7):4511–27. doi: 10.5194/acp-16-4511-2016.

- Zhang, Jie, Manish Shrivastava, Lan Ma, Wenqing Jiang, Cort Anastasio, Qi Zhang, and Alla Zelenyuk. 2024. "Modeling Novel Aqueous Particle and Cloud Chemistry Processes of Biomass Burning Phenols and Their Potential to Form Secondary Organic Aerosols." *Environmental Science and Technology* 58(8):3776–86. doi: 10.1021/acs.est.3c07762.
- 695 Zhang, Qi, and Cort Anastasio. 2001. "Chemistry of Fog Waters in California's Central Valley—Part 3: Concentrations and Speciation of Organic and Inorganic Nitrogen." *Atmospheric Environment* 35(32):5629–43. doi: https://doi.org/10.1016/S1352-2310(01)00337-5.

- Zhang, Qi, and Cort Anastasio. 2003a. "Conversion of Fogwater and Aerosol Organic Nitrogen to Ammonium, Nitrate, and NOx during Exposure to Simulated Sunlight and Ozone." *Environmental Science & Technology* 37(16):3522–30. doi: 10.1021/es034114x.
- Zhang, Qi, and Cort Anastasio. 2003b. "Free and Combined Amino Compounds in Atmospheric Fine Particles (PM2.5) and Fog Waters from Northern California." *Atmospheric Environment* 37(16):2247–58. doi: https://doi.org/10.1016/S1352-2310(03)00127-4.
- Zhang, Qi, Cort Anastasio, and Mike Jimenez-Cruz. 2002. "Water-Soluble Organic Nitrogen in Atmospheric Fine Particles (PM2.5) from Northern California." *Journal of Geophysical Research: Atmospheres* 107(D11):AAC 3-1-AAC 3-9. doi: https://doi.org/10.1029/2001JD000870.
 - Zhang, Qi, Jose L. Jimenez, Manjula R. Canagaratna, Ingrid M. Ulbrich, Nga L. Ng, Douglas R. Worsnop, and Yele Sun. 2011. "Understanding Atmospheric Organic Aerosols via Factor Analysis of Aerosol Mass Spectrometry: A Review." *Analytical and Bioanalytical Chemistry* 401(10):3045–67. doi: 10.1007/s00216-011-5355-y.
- 710 Zhao, Y., A. G. Hallar, and L. R. Mazzoleni. 2013. "Atmospheric Organic Matter in Clouds: Exact Masses and Molecular Formula Identification Using Ultrahigh-Resolution FT-ICR Mass Spectrometry." Atmos. Chem. Phys. 13(24):12343–62. doi: 10.5194/acp-13-12343-2013.